Available online at www.sciencedirect.com
ScienceDirect
Journal of Magnetism and Magnetic Materials 320 (2008) e275–e278
Journal of magnetism and magnetic materials
www.elsevier.com/locate/jmmm

# Reversible and irreversible magnetization components behavior in Ni nanowires

C. Rocha, T.R.F. Peixoto, D.R. Cornejo*

*Instituto de Física, Universidade de São Paulo, 05508-900 São Paulo, SP, Brazil*

Available online 21 February 2008

**Abstract**

Polycrystalline Ni nanowires were electrodeposited in nanoporous anodized alumina membranes with mean diameter of approximately 42 nm. Their magnetic properties were studied at 300 K, by measurements of recoil curves from demagnetized state and also from saturated state. $M_{rev}$ and $M_{irr}$ components were obtained and $M_{rev}(M_{irr})_H$ curves were constructed from the experimental data. These curves showed a behavior that suggests a non-uniform reversal mode influenced by the presence of dipolar interactions in the system. A qualitative approach to this behavior is obtained using a Stoner–Wohlfarth model modified by a mean field term and local interaction fields.


*PACS:* 75.60.Ej; 75.60.Jk; 75.75.+a

*Keywords:* Ni nanowire; Magnetization reversal; Irreversible magnetization; Magnetic interaction

## 1. Introduction

Recently, patterned nanowire structures have been intensively studied due to their potential application in high-density recording media and microelectromechanical systems [1]. One simple method to obtain self-organized arrays of nanowires is using anodized alumina membranes (AAMs) as templates [2]. These templates can be homogeneously filled with magnetic elements such as Ni by means of a well-controlled electrodeposition process.

The magnetization process in these materials offers interesting challenges, since the interplay between the different anisotropies favors soft magnetic material like Ni to display coercivities comparable to hard magnetic materials.

To study mechanisms of magnetization reversal, it is common to separate the total magnetization $M$ into reversible ($M_{rev}$) and irreversible ($M_{irr}$) components. $M_{irr}$ can be experimentally probed by measuring remanence curves from the demagnetized state (i.e., the isothermal remanence, $M_{irr} = M_r(H_p)$) and from the saturated state (obtaining the demagnetization remanence, $M_{irr} = M_d(H_p)$), for a set of return fields $H_p$. Thus, $M_{rev}(H_p, H)$ of any state of magnetization is immediately defined as $M_{rev} = M - M_{irr}$. By using a suitable set of first-order reversal curves, it is possible to build, for several values of the magnetic internal field $H$, $M_{rev}(M_{irr})_H$ curves. The behavior of these curves gives an indicative of the magnetization reversal mode of the material [3]. For systems that reverse by coherent rotation, $M_{rev}(M_{irr})_H$ curves are linear, with negative slope. On the other hand, in systems whose reversal mechanism is domain wall unpinning or nucleation of inverse domains, these curves are parabolic, exhibiting a minimum during demagnetization process.

In a previous work [4], a new form of $M_{rev}(M_{irr})_H$ curves was reported in Fe nanowires. In this work, we report a similar behavior of these curves for Ni nanowire arrays and a qualitative approach of this behavior by means of computational modeling. We generated numerical first-order recoil curves through an interacting Stoner–Wohlfarth model and obtained $M_{rev}(M_{irr})_H$ by the same way as the experimental curves. This model is based in one originally developed by Crew [5,6] and it takes into

*Corresponding author. Tel.: +55 11 3091 6885; fax: +55 11 3091 6984.
*E-mail address:* cornejo@if.usp.br (D.R. Cornejo).

0304-8853/$ - see front matter © 2008 Elsevier B.V. All rights reserved.
doi:10.1016/j.jmmm.2008.02.058

account a mean field proportional to the total magnetization and a log-normal distribution of local interaction fields, with mean zero.

## 2. Experimental details

The samples were synthesized by the following procedure. Aluminum foils (99.997%) were cleaned in solution of acetone and electropolished in $H_3PO_4 + H_2SO_4 + H_2O$ solution (4:4:2 weight), at 20 V dc. The first anodization was carried out at ~4 °C, in a bath of $C_2H_2O_4$ (0.3 M) by 1 h, at 20 V dc. The initial $Al_2O_3$ membrane was removed in acidic 0.2 M $CrO_3 + 0.4$ M $H_3PO_4$ solution at 50 °C during 40 min. The second anodization was carried out in the same conditions during 40 min. The nanowires of Ni were deposited inside the porous membrane by an ac electrodeposition at 20 V, 100 Hz and using an electrolyte containing $NiSO_4 \cdot 6H_2O$ (0.1 M), and 45 g/L $H_3BO_3$, for 2 min. The structural characterization was done by Atomic Force Microscopy (AFM), Magnetic Force Microscopy (MFM) and X-ray Diffractometry (XRD) with Cu-$K_\alpha$ radiation ($\lambda = 1.5418$ Å). The magnetic measurements were carried out at 300 K, in a Quantum Design$^{TM}$ 7T-SQUID, with magnetic field perpendicularly applied to the membrane surface.

## 3. Structural and magnetic characterization

AFM and MFM micrographs were obtained after the electrodeposition and a subsequent field application in order to align any magnetic domains perpendicularly to the surface. In Fig. 1, we show AFM (left) and MFM (right) images with 1 μm scan size. We can clearly observe a highly oriented hcp pore growth pattern and the conformation between surface topology and magnetic domains with perpendicular orientation. From these images, we estimated the mean diameter of pores, which turns out to be about 42 nm for anodization voltage of 20 V.

The XRD results (not shown here by reason of space) corroborate the MFM results and confirm the presence of polycrystalline Ni in the samples. The diffractogram showed also strong peaks of Al substrate absence of $Al_2O_3$ peaks suggesting that it is amorphous. The (1 1 1) Ni peak was not observed because it coincides with the strong (2 0 0) Al peak. For the fcc structure, the (1 1 1) peak should be the strongest, so we cannot conclude that [2 2 0] is the preferential direction of growth. The grain size in the direction [2 2 0] was calculated by Scherrer formula, resulting in approximately 17 nm.

For the magnetic characterization, we obtained $M_r(H_p)$ and $M_d(H_p)$ from measurements of remanence curves (described elsewhere [7]) at 300 K. The coercivity was $H_C = 562$ Oe. In Fig. 2a, we compare the behavior of remanent (irreversible) magnetizations during the initial magnetization process and the demagnetization from saturation. At equal values of field, the later is always larger than the first, due to the magnetic ordering created in saturated state. We plotted $M_{rev}(M_{irr})_{H_p}$ curves in Fig. 2b for several values of $H_p$. Remarkably, the form of these curves is very different from known materials that reverse by coherent rotation (straight lines) or nucleation and unpinning of reversal domains (parabolic curves) [3]. This suggests that these curves could be associated with some non-uniform reversal mode, once the single-domain magnetic grains must be of the same size as the grain size results from XRD analysis.

## 4. Discussion

We reproduced qualitatively the experimental results through a numerical micromagnetic model. We applied an interacting Stoner–Wohlfarth model developed by Crew [5,6]. In the Stoner–Wohlfarth model, the free energy density of a uniaxial single-domain particle of volume $V$, in the presence of magnetic field $H$ is given by $E/V = K_{eff} \sin^2(\Psi - \theta) - M_S H \cos \Psi$, where $K_{eff}$ is the

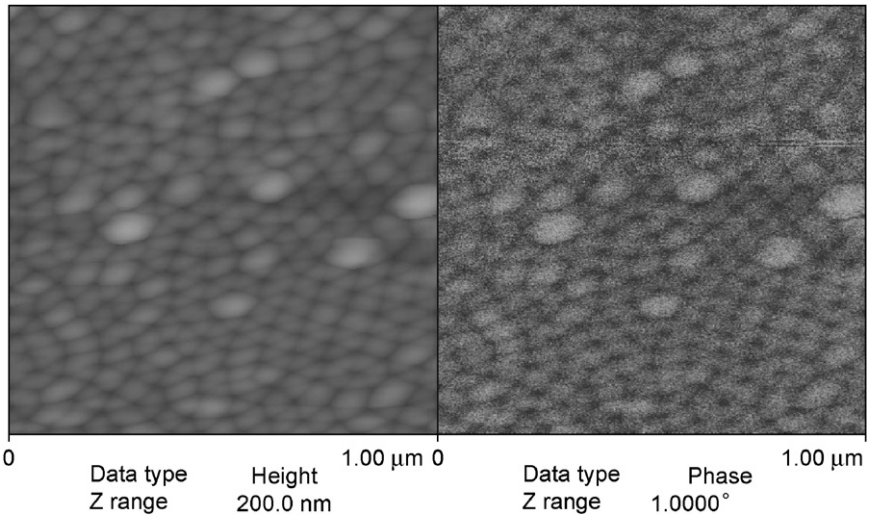


Fig. 1. AFM (left) and MFM (right) micrographs for the sample studied.

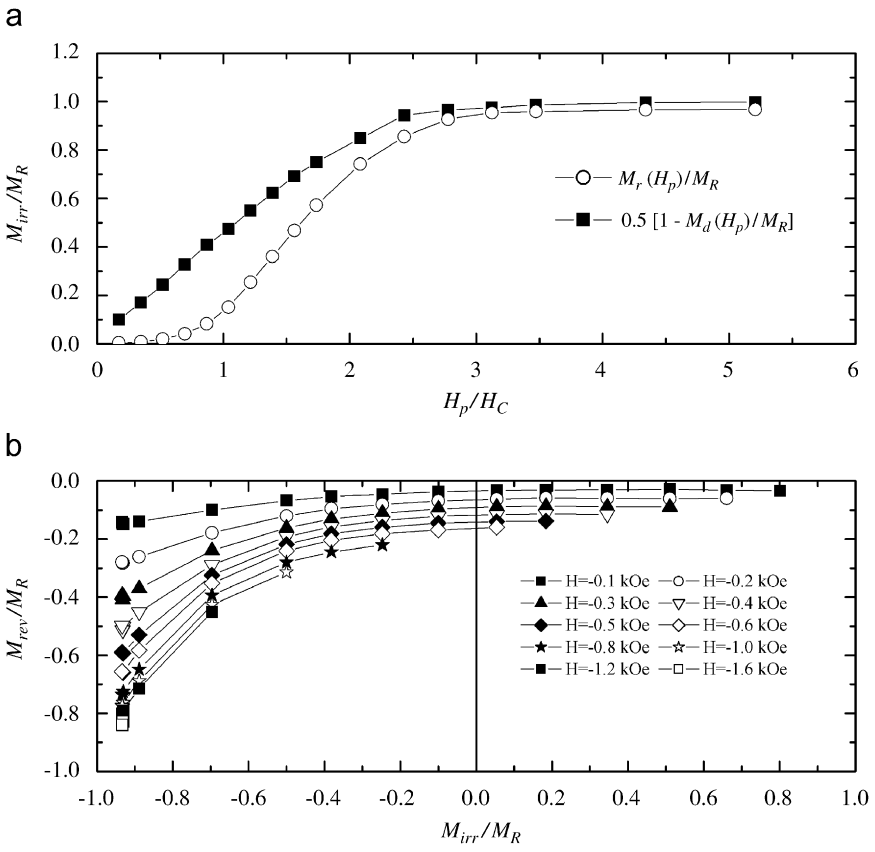


Fig. 2. (a) Normalized $M_{\rm irr}$ functions for the initial magnetization curve (circles) and the demagnetization curve (squares); (b) $M_{\rm rev}(M_{\rm irr})_H$ at different values of $H$, for a sample with $H_C = 562\,\mathrm{Oe}$.

effective anisotropy constant, $M_S$ is the saturation magnetization, $\Psi$ is the angle between particle's moment and the magnetic field and $\theta$ is the angle between the magnetic field and the particle's easy-axis.

We determine the critical angles $\Psi_1$, $\Psi_2$, $\Psi_3$, where $\Psi_1$ and $\Psi_3$ are the minima and $\Psi_2$ is a maximum between them. Then, we calculate the total magnetization for an ensemble of single-domain particles with a log-normal distribution of volumes and a random isotropic distribution of easy-axis orientations, at an applied field $H_a$ and a time $t$, which is given by

$$M_{\rm tot}(H_a, t) = \int_{-\infty}^{+\infty} N(\Delta_i) M(H_{\rm tot}, t)\, \mathrm{d}\Delta_i, \tag{1}$$

where $N(\Delta_i)$ is a normal distribution of local interaction fields with mean zero and standard deviation $\sigma$. $H_{\rm tot}$ is the effective field and it is given by $H_{\rm tot} = H_a + \alpha M_{\rm tot}(H_a, t) + \Delta_i$ where $\alpha$ is an adimensional constant that determines the strength of the mean field and $M(H_{\rm tot}, t)$ is given by

$$M(H_{\rm tot}, t) = \int_0^{\pi/2}\int_0^{\infty} \sin\theta V f(V) P(\theta, V, H, t) \cos\Psi_1\, \mathrm{d}V\, \mathrm{d}\theta + \int_0^{\pi/2}\int_0^{\infty} \sin\theta V f(V)[1 - P(\theta, V, H, t) \times \cos\Psi_3]\, \mathrm{d}V\, \mathrm{d}\theta. \tag{2}$$

In Eq. (2), $f(V)\,\mathrm{d}V$ is the number of particles with volumes between $V$ and $V+\mathrm{d}V$. $f(V)$ is a log-normal distribution, with mean $V_m$ and standard deviation $\sigma_V = 1$ and $P(\theta, V, H_{tot}, t)$ is the population distribution of particles in a given minimum. $P(\theta, V, H_{\rm tot}, t)$ is given by $P(\theta, V, H_{\rm tot}, t) = R/Q + W\exp\{-Qt\}$, where $R = 1/\tau_2$ and $Q = 1/\tau_1 + 1/\tau_2$ and $\tau_1$ and $\tau_2$ are the thermal relaxation times for minima $\Psi_1$ and $\Psi_3$, respectively, and $W = P(0) - R/Q$. The time constant $\tau$ for decay over an energy barrier $\Delta E$ is given by $\tau^{-1} = f_0 \exp(-\Delta E/k_B T)$.

In our simulations, we considered $t = 100\,\mathrm{s}$ because we assumed that $H_a$ is independent of time, so that the time of measurement is large enough for particles to attain equilibrium. The set of parameters that best fits the experimental behavior of $M_{\rm rev}(M_{\rm irr})_H$ was $\alpha = 0.80$, standard deviation (of $\Delta_i$) $\sigma = 750\,\mathrm{Oe}$, mean volume $V_m = 4.188 \times 10^{-18}\,\mathrm{cm}^3$, $M_S = 6.2 \times 10^3\,\mathrm{emu/cm}^3$ (value corresponding to Ni bulk) and $K_{\rm eff} = 100 K_1$ of Ni bulk. This set of parameters yields the curves shown in Fig. 3. These plots correspond to the same plots in Fig. 2.

The numerical results represent the experimental curves well qualitatively. In Fig. 3a, the difference on the behavior of the two curves shows that the irreversible magnetization is sensitive to the initial state of the system, namely the demagnetized state (circles) and the saturated state (squares). This magnetic memory arises from the dipolar

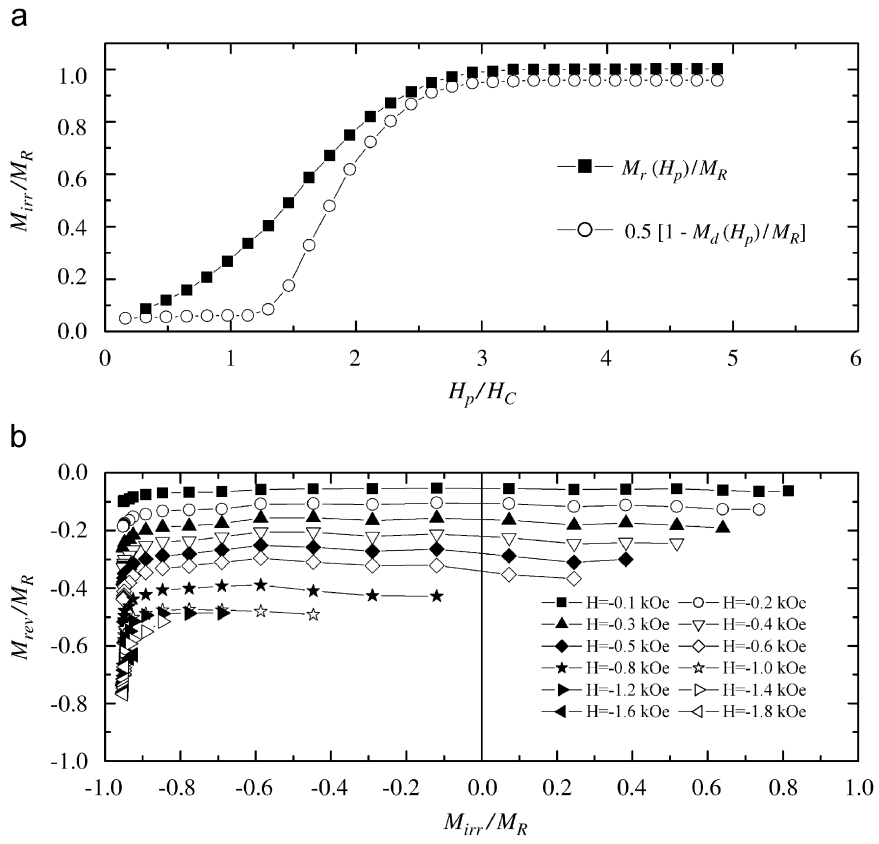


Fig. 3. Numerical $M_{\mathrm{rev}}(M_{\mathrm{irr}})_H$ for several values of $H$.

interactions between particles, which tend to align each other. These interactions are modeled by the mean field term and the distribution of local interaction fields. The effect of the dipolar field depends on the geometry of the particles, since it can enhance or diminish the effect of the applied field. In our simulations, we did not make any considerations about the shape of the particles. However, it is reasonable that $K_{\mathrm{eff}} = 100K_1$, because the shape anisotropy should be dominant in the wires.

In Fig. 3b, we plot the numerical $M_{\mathrm{rev}}(M_{\mathrm{irr}})_H$ curves. Qualitatively, this plot is in reasonable accord with the results from Fig. 2b. For positive values of $M_{\mathrm{irr}}$, the corresponding $M_{\mathrm{rev}}$ remains practically constant. However, at negative and increasing values of $M_{\mathrm{irr}}$, $M_{\mathrm{rev}}$ increases. The values of $M_{\mathrm{irr}}$ become negative when $H < -600$ Oe, approximately, and $M_{\mathrm{rev}}$ increases monotonically at $H \leqslant -1.4$ kOe.

Thus, we modeled the magnetization reversal mode of Ni nanowires through an ensemble of single-domain interacting particles, in a mean field description with local interactions fields. The numerical results reproduce qualitatively the experimental behavior of irreversible magnetization curves, both in the demagnetization from saturated state and magnetization from demagnetized state. The curves from Figs. 2b and 3b may be associated to some non-uniform reversal mode [4], since the single-domain particles interact through long-range dipolar fields.

## Acknowledgments

We wish to acknowledge that this work was partially supported by CNPq, CAPES and FAPESP.

## References

[1] C.N.R. Rao, F.L. Deepak, G. Gundiah, A. Govindaraj, Prog. Solid State Chem. 31 (2003) 5.
[2] H. Masuda, K. Fukuda, Science 268 (1995) 1466.
[3] D.C. Crew, P.G. McCormick, R. Street, J. Appl. Phys. 86 (1999) 3278.
[4] D.R. Cornejo, E. Padrón-Hernández, J. Magn. Magn. Mater. 316 (2007) e48.
[5] D.C. Crew, Ph.D. Thesis, The University of Western Australia, 1998.
[6] D.C. Crew, S.H. Farrant, P.G. McCormick, R. Street, J. Magn. Magn. Mater. 163 (1996) 299.
[7] M. Emura, D.R. Cornejo, F.P. Missell, J. Appl. Phys. 87 (2000) 1387.